Neurones associated with saccade metrics in the monkey central mesencephalic reticular formation

Jason A. Cromer[1,2] and David M. Waitzman[1,2]

University of Connecticut Health Center, [1]Department of Neurology and [2]Program in Neuroscience, 263 Farmington Avenue, Farmington, CT 06030, USA

Neurones in the central mesencephalic reticular formation (cMRF) begin to discharge prior to saccades. These long lead burst neurones interact with major oculomotor centres including the superior colliculus (SC) and the paramedian pontine reticular formation (PPRF). Three different functions have been proposed for neurones in the cMRF: (1) to carry eye velocity signals that provide efference copy information to the SC (feedback), (2) to provide duration signals from the omnipause neurones to the SC (feedback), or (3) to participate in the transformation from the spatial encoding of a target selection signal in the SC into the temporal pattern of discharge used to drive the excitatory burst neurones in the pons (feed-forward). According to each respective proposal, specific predictions about cMRF neuronal discharge have been formulated. Individual neurones should: (1) encode instantaneous eye velocity, (2) burst specifically in relation to saccade duration but not to other saccade metrics, or (3) have a spectrum of weak to strong correlations to saccade dynamics. To determine if cMRF neurones could subserve these multiple oculomotor roles, we examined neuronal activity in relation to a variety of saccade metrics including amplitude, velocity and duration. We found separate groups of cMRF neurones that have the characteristics predicted by each of the proposed models. We also identified a number of subgroups for which no specific model prediction had previously been established. We found that we could accurately predict the neuronal firing pattern during one type of saccade behaviour (visually guided) using the activity during an alternative behaviour with different saccade metrics (memory guided saccades). We suggest that this evidence of a close relationship of cMRF neuronal discharge to individual saccade metrics supports the hypothesis that the cMRF participates in multiple saccade control pathways carrying saccade amplitude, velocity and duration information within the brainstem.

(Received 17 August 2005; accepted after revision 23 November 2005; first published online 24 November 2005)
Corresponding author D. M. Waitzman: Department of Neurology, MC 3974, 263 Farmington Avenue, Farmington, CT 06030, USA. Email: waitzman@nso2.uchc.edu

The purpose of the saccadic system is to rapidly shift the eyes to point the fovea toward targets of interest. The amplitude and direction of the intended target of an upcoming gaze shift is encoded by activation of a particular locus of neurones in the deep layers of the superior colliculus (SC) (Wurtz & Goldberg, 1972; Sparks, 1975; Freedman & Sparks, 1997). By virtue of their position in the SC motor map (a spatial code), this population of active SC neurones provides a vector representation of the *target's* location relative to the current position of gaze. While the theoretical issues surrounding the transformation of this target selection signal into motor output have been identified (for reviews, see Sparks & Mays, 1990; Sparks, 1999, 2002), the neural elements that carry out these processes remain unclear.

One brain region that could participate in the generation of movement commands from the collicular target selection signal is the central mesencephalic reticular formation (cMRF). It receives strong, topographical projections from the SC (Cohen & Büttner-Ennever, 1984; Moschovakis *et al.* 1988*a*; Chen & May, 2000). In addition, it provides descending projections to the omnipause neurones (OPNs), the excitatory burst neurones (EBNs), and the inhibitory burst neurones (IBNs) in the pons (Büttner-Ennever, 1988; Langer & Kaneko, 1990; Scudder *et al.* 1996). Based on these descending anatomical connections, the cMRF is a good candidate to participate in a feed-forward transformation of the collicular output into temporal signals. At the same time, evidence of reciprocal connections with the SC (Moschovakis *et al.* 1988*b*; Chen & May, 2000) and OPNs (Langer & Kaneko, 1983) suggests that the cMRF could also mediate the feedback of ongoing saccade dynamics to the SC (Waitzman *et al.* 1996; Soetedjo *et al.* 2002).

 DOI: 10.1113/jphysiol.2005.096834

Three physiological studies have made specific predictions about the functions of the cMRF in saccade control. Waitzman *et al.* (1996) found that a subset of cMRF neurones were associated with eye velocity and hypothesized that these signals were fed back to the SC. One drawback of this study was that a template-matching algorithm was used to examine the relationship of cell discharge to eye velocity. This approach normalized both peak eye velocity and saccade duration. Thus, no distinction could be made between cells encoding just peak eye velocity from those cells encoding instantaneous eye velocity for the duration of the saccade. Furthermore, no behavioural mechanism was used to control saccade dynamics. As a result, no definitive test was performed to decide if the discharge of cMRF neurones varied with changes in saccade velocity or duration.

A second feedback function of the cMRF was suggested by Soetedjo *et al.* (2002). They proposed that the afferent input to the cMRF from the OPNs and efferent output to the SC make it an ideal candidate to provide duration information that sustains the SC target selection signal for the entire saccade. They predicted that the discharge of individual cMRF neurones would have an isolated relationship to saccade duration and not to other saccade metrics. Most previous studies of the cMRF have either not examined the relationship between saccade and burst duration or have found that no such relationship exists (Moschovakis *et al.* 1988*b*). In the cases where cMRF neurones with a duration relationship were reported, the neurones were also related to other saccade metrics (Handel & Glimcher, 1997; Pathmanathan *et al.* 2005*a*). Thus, to date no neurones in the cMRF with solely a duration relationship have been identified.

A third report (Pathmanathan *et al.* 2005*a*) postulates that cMRF neurones could participate in the development of temporally coded excitatory burst neurone signals from the spatially coded SC target selection signal. The input of the proposed three layer model was purely spatial (representing the SC). Based on the pattern of connections and synaptic weightings, this model developed temporally coded signals similar to those found in PPRF medium lead burst neurones in the output layer (Pathmanathan & Waitzman, 2003). The model predicted that neurones in the intermediate layer would have a variety of relationships to saccade dynamics. Furthermore, some of the neurones in this model would be associated with peak eye velocity while others would be associated with saccade duration. Thus, if cMRF neurones mimic the cells in the middle layer of this model, they would display a spectrum of relationships to various saccade metrics that ranged from very weak to strong.

The predictions of these three studies suggest that a careful re-examination of the metrics of cMRF neuronal discharge and its variation during a wider range of saccade dynamics is required. To this end, we analysed the discharge of cMRF neurones for evidence of specific relationships to saccade metrics. In order to increase the dynamic range of saccade parameters, we had monkeys perform visually guided (VG), memory guided (MG), and spontaneous saccades in total darkness. MG saccades have a lower peak velocity and longer duration than VG saccades of the same amplitude and direction (Hallett & Lightstone, 1976). If the discharge of neurones in the cMRF is correlated to saccade metrics then the firing of these neurones should change in direct correspondence with the changes in saccade duration and peak velocity observed during VG and MG saccades. Thus, using this approach we should be able to identify whether cMRF neurones with the appropriate activity hypothesized by the above models exist. Preliminary accounts of these results have been presented previously in abstract form (Cromer *et al.* 2003, 2004).

Methods

Surgical preparation and cMRF isolation

Two adult, male rhesus monkeys were prepared for single neurone recording in the cMRF. All experiments were approved by the Animal Care and Use Committee of the University of Connecticut Health Center and complied with the principles enunciated in the 'Guide for the Care and Use of Laboratory Animals' (NIH publication no. 86-23, revised 2001). Animals were primed for surgery using atropine (0.04 mg kg^{-1}, I.M.) and ketamine (15 mg kg^{-1}, I.M.), followed by general inhalational anaesthesia using isoflurane (1–2%) in conjunction with 100% oxygen (1 l min^{-1}). Once a stable plane of anaesthesia was achieved (judged by lack of corneal response and loss of the withdrawal reflex to toe pinch), a scleral search coil was implanted under the conjunctiva of one eye (Robinson, 1963; Judge *et al.* 1980). A sagittal incision was made over the skull and a stainless steel recording chamber (angle 0 deg) was stereotactically placed over a midline trephine hole (A3.0) allowing access to both cMRFs. The chamber, a head fixation device, and the connector for the search coil were fixed in position using dental acrylic and vitalium bone screws arrayed around the skull. Analgesics (buprenorphine, 1 mg kg^{-1} I.M. every 6 h for 48 h post-operatively and then as needed) and antibiotics (cefazolin, 33 mg kg^{-1} I.V. 1 h prior to start of surgery followed by 33 mg kg^{-1} I.M. every 12 h for 3 days following surgery) were administered to control post-surgical pain and infection.

After the monkey was trained to criterion on the behavioural tasks (90%), localization of the cMRF began. The oculomotor nucleus was identified by the characteristic burst-tonic discharge of its neurones and

confirmed by low current electrical stimulation which induced movement only in the ipsilateral eye (except upward). Care was taken to confirm the approximate depth of the top of the oculomotor nucleus both by unit recording and by electrical stimulation. cMRF neurones were then isolated 2–4 mm lateral to the oculomotor nucleus at a depth ranging from 3 mm above the top of the oculomotor nucleus to 3 mm below the top of the nucleus. We localized cMRF neurones along the entire rostral to caudal extent of the oculomotor nucleus.

At the conclusion of experiments, microbeads (Lumiflor) were injected at known locations relative to our recording sites. Animals were euthanized by induction of deep anaesthesia using sodium pentobarbital (100 mg kg^{-1}, I.P.) followed by perfusion with 4% paraformaldehyde and 0.1% glutaraldehyde. Anatomical reconstruction identified the position of the beads and of the oculomotor nuclei. These reference points were then used to determine the location of recorded neurones in the cMRF.

Behavioural protocols

Monkeys were trained to perform both visually guided (VG) and memory guided (MG) saccades with the head restrained. Each trial started with an ∼1000 ms period of fixation followed by the presentation of a peripheral visual target. In the VG overlap task, the monkey was cued to make a saccade to the still visible target by the offset of the fixation point. In the MG task, the target light was flashed for 250 ms. The monkey was cued to make a MG saccade to the location of the previously flashed target by the offset of the fixation point 500–1000 ms later.

For all experiments, the fixation spot was always presented at primary position in order to avoid the influence of initial eye position in the orbit (i.e. reference frame effects). Each trial consisted of a single VG or MG movement to an eccentric target. We positioned targets (up to ± 30 deg around primary position) to obtain a complete movement field within our range of recording. One of the two monkeys rarely performed saccade amplitudes greater than 25 deg. As a result, the sizes of the movement fields for the neurones recorded from this monkey were smaller.

Data analysis

All cells localized to the cMRF that were identified during recording as having burst or build-up activity related to saccades were included in the analysis as long as at least 500 saccades were collected while recording the neurone (60 cells). Implementation of this saccade number criterion increased the likelihood that we had obtained a complete movement field for each of the cells. The start of a saccade was marked when the eye velocity exceeded 15 deg s^{-1} and the end of the saccade was identified as the time when the velocity fell below that level. For each saccade, we counted the number of spikes (NOS) across the interval from 100 ms prior to saccade onset to 10 ms after the end of the saccade. This interval was chosen because saccade-associated activity in the cMRF had previously been demonstrated to occur in this timeframe (Moschovakis *et al.* 1988*b*; Waitzman *et al.* 1996). To avoid a biased NOS count in cMRF neurones with a high background rate of activity, we calculated the background firing level for each neurone during non-trial periods (in complete darkness) at times when no saccades were being made and subtracted the corresponding NOS from the counts (Waitzman *et al.* 1996). This prevented an artificial inflation of the NOS counted for larger saccades, which have a longer duration and therefore a longer counting interval.

Movement field plots were constructed for each neurone as previously described (Pathmanathan *et al.* 2005*b*). These plots display average spike number as a function of saccade direction and amplitude as if the eyes had started at primary position (i.e. retinotopic coordinates). While VG and MG saccades were initiated from primary position, most spontaneous saccades were not. This explains why some movement fields display saccades with amplitudes larger than the maximum target displacement we tested (±30 deg). For example, if the monkey made a saccade from −20 deg to +20 deg, this would appear on the movement field as a +40 deg saccade (assuming enough saccades of similar amplitude were collected, $n = 3$).

A cell's optimal direction was calculated by testing reference directions from 0 to 359 deg at 1 deg intervals as described by Moschovakis *et al.* (1988*b*). Briefly, the component amplitude in the reference direction for all saccades within ±90 deg of the reference direction was computed. The optimal direction was selected as the reference direction where linear regression analysis between the component amplitudes and NOS had the highest correlation.

An iso-direction set was obtained by selecting saccades within ±15 deg of the cell's optimal direction and was used for all subsequent analysis. The peak firing rate of the cell was determined for each saccade based on the peak firing rate during the same interval used to count the NOS (100 ms before to 10 ms after the saccade). A spike density function was created by convolving the unit activity with a Gaussian ($\sigma = 10$ ms) (MacPherson & Aldridge, 1979; Silverman, 1986). Neuronal bursts were identified independently of saccades in a three-step process. The mean firing rate across the entire recording of the neurone was determined first. Burst locations were then detected based on when a smoothed version of the spike density function (moving average filter, 15 point parabolic, centre weighted) exceeded the mean firing rate by two standard deviations. From these points, the onset and offset of the bursts where found by moving forward (offset) and

backwards (onset) until the smoothed spike density fell below one standard deviation above the mean firing rate. Note that the smoothing process was used *only* to establish the time points of burst onset and offset in an objective fashion. The unaltered spike density function was used for all other data analysis and figure displays.

We then analysed the discharge of cMRF neurones for evidence of three metrical relationships: number of spikes *versus* saccade amplitude (amplitude), peak saccade velocity *versus* peak firing rate (peak), and saccade duration *versus* burst duration (duration). Duration relationships were examined for the set of saccades that matched the independently identified neuronal burst. To identify whether the population of neurones fell into different groups based on the contribution of the three metrical relationships each cell possessed, we performed both hierarchical and k-means clustering analysis (Hartigan, 1975) using the Matlab Statistical Toolbox (Mathworks). We first performed a hierarchical clustering using Euclidean distances and Ward's methods of amalgamation (Ward & Neel, 1970). To determine if other hierarchical methods better fitted the data, we employed a comparison of cophenetic correlation coefficients as a measure of how well the hierarchical tree accounted for dissimilarities among individual data points (Matlab 'cophnet' function). By maximizing the cophenetic correlation coefficient, we chose distance and amalgamation routines that best fitted our data and thereby best defined the number of clusters into which the data should be placed. When performing k-means clustering, we estimated the optimal number of clusters by comparing silhouette values. A value close to 1.0 is obtained when the average distance from a data point to the other data points within its own cluster is smaller than the average distances to all data points in the closest cluster. On the other hand, a silhouette value close to zero indicates that the data point could equally well have been assigned to the neighbouring cluster. A negative silhouette is obtained when the cluster assignment has been arbitrary (Rousseeuw, 1987). Therefore, we picked the number of k-means clusters by minimizing the number of negative silhouette values and maximizing the mean silhouette value. Agreement of the optimal number of clusters identified by the hierarchical and k-means clustering methods would suggest an appropriate grouping of data.

Finally, a dynamic analysis was performed on the iso-direction set for *only* those neurones that displayed one of the tested metrical relationships (Cullen *et al.* 1996). The model utilized for our population was based on eye velocity ($\dot{E}$):

$$FR(t) = a + b \times \dot{E}(t + td) \quad (1)$$

Models were created by inputting the recorded eye velocity, shifting it in time by *td* (representing the time delay, or latency, from neuronal activity to movement), scaling it by parameter *b* (gain), and summing it with parameter *a* (bias). For each neurone, the model parameters were optimized using a linear least squares method. The goodness of fit between the model and actual firing rate was assessed by the Variance Accounted For (VAF). We chose to examine a velocity model because our previous study in head-unrestrained monkeys found that most cMRF neurones were best fitted by this model (Pathmanathan *et al.* 2005*a*) and because the same model has been found to best represent the discharge of IBNs (Cullen & Guitton, 1997).

Results

General discharge characteristics

In general, the discharge of the 60 cMRF neurones reported here began before and continued throughout saccades. For example, the discharge of the neurone shown in Fig. 1 began to slowly rise as early as 100 ms before contraversive saccades (25 deg target) and then generated a tightly coupled burst of firing that started ~20–50 ms before saccade onset (Fig. 1*C*). This pattern of discharge suggested that these were long-lead burst neurones (Luschei & Fuchs, 1972; Hepp & Henn, 1983). A majority of the neurones had large, open movement fields for which the number of spikes increased monotonically with movement amplitudes (Fig. 2, first column). These cells were usually active for all eye movements with a component of movement in a primary cardinal direction (left, right, up or down) and for those cells which were horizontally tuned, the firing was predominantly contraversive. Figure 2 shows five cells that displayed this characteristic activation for all saccades in a cardinal direction.

Some neurones were also documented with movement fields that were closed (i.e. had activity only for movements of a limited set of amplitudes and directions) (e.g. see Wurtz & Goldberg, 1972; Sparks, 1975; Waitzman *et al.* 1996; Pathmanathan *et al.* 2005*b*) or for which spike number reached a plateau or declined beyond a certain amplitude, called non-monotonic open movement fields (e.g. see Moschovakis *et al.* 1988*a*; Munoz & Wurtz, 1995; Pathmanathan *et al.* 2005*b*). We also found a previously undocumented group of cells (about one fifth of the total) that had relatively low saccade-associated discharge. The movement fields of these neurones had no discernable pattern.

In addition to their movement field properties, the saccade-associated burst for each cMRF neurone displayed up to three additional relationships to the metrics of saccades that permitted further categorization. All three relationships were qualitatively evident in the discharge of the tightly coupled saccade-related neurone displayed in Fig. 1. First, the number of spikes in the saccade-associated

burst increased monotonically with amplitude (Fig. 1*A*, note the increased spike number with amplitude, 3rd row). Second, peak firing rate increased monotonically with peak saccade velocity (Fig. 1*A–C*) up to the point at which the peak velocity saturated. Third, burst duration was monotonically associated with saccade duration (Fig. 1*A–C*). These relationships were then explored quantitatively across the entire sample of cMRF neurones.

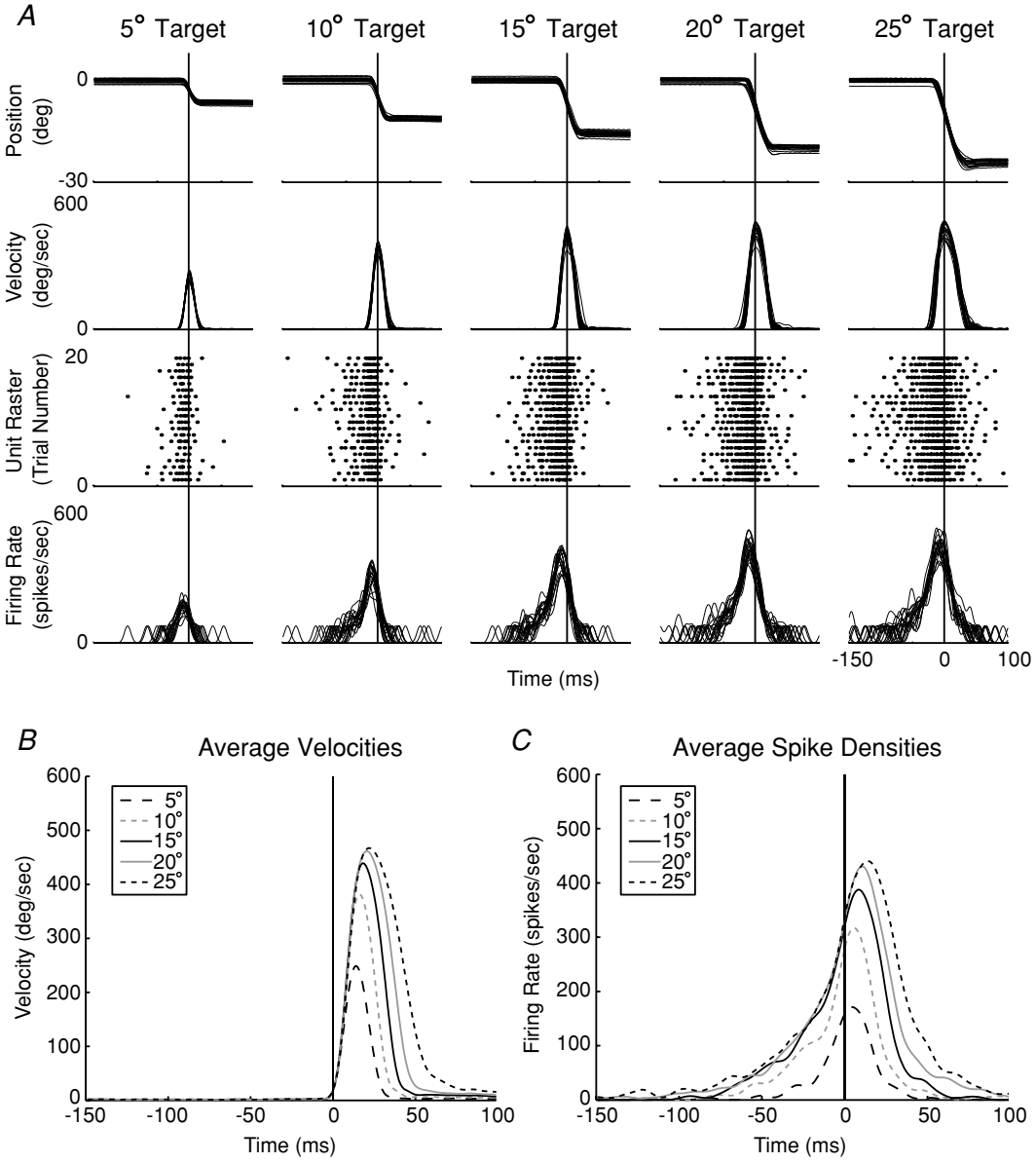

Figure 1. cMRF neurone tightly coupled to eye movement
A, sample eye position, eye velocity, unit raster and spike densities traces (respective rows from top to bottom) for contraversive visually guided saccades made to progressively larger leftward targets (20 trials for each target, individual trials shown overlaid). All trials are aligned on peak saccade velocity (vertical lines). Saccade trajectories and velocities to individual targets are similar, showing little variance. Saccade velocity increases for progressively larger targets up to ~20 deg where it begins to saturate (peak velocities for 20 deg or 25 deg targets are similar). The number of spikes generated by the neurone increased for larger saccades. Likewise, the peak discharge and burst duration for larger saccades increased in conjunction with similar increases in peak velocity and saccade duration. *B*, the average velocities for all trials to each target, realigned on saccade onset. Note the clear increase in saccade velocity and duration for larger saccades. *C*, average spike densities for saccades to each target, aligned on saccade onset (vertical line), demonstrate that the neuronal discharge mirrors the relationship to peak velocity and duration, even when peak velocity begins to saturate. Long-lead activity begins ~100 ms before the largest saccades and robust burst activity proceeds saccade onset by ~20–50 ms.

Relationship to saccade metrics

Figure 2 (right three columns) shows scatter plots of the three metrical relationships we examined for five representative cMRF neurones. In total, 82% of the neurones we examined were correlated with at least one of three saccade metrics ($n = 49$). The relationships to each of the saccade metrics for all of the neurones are shown

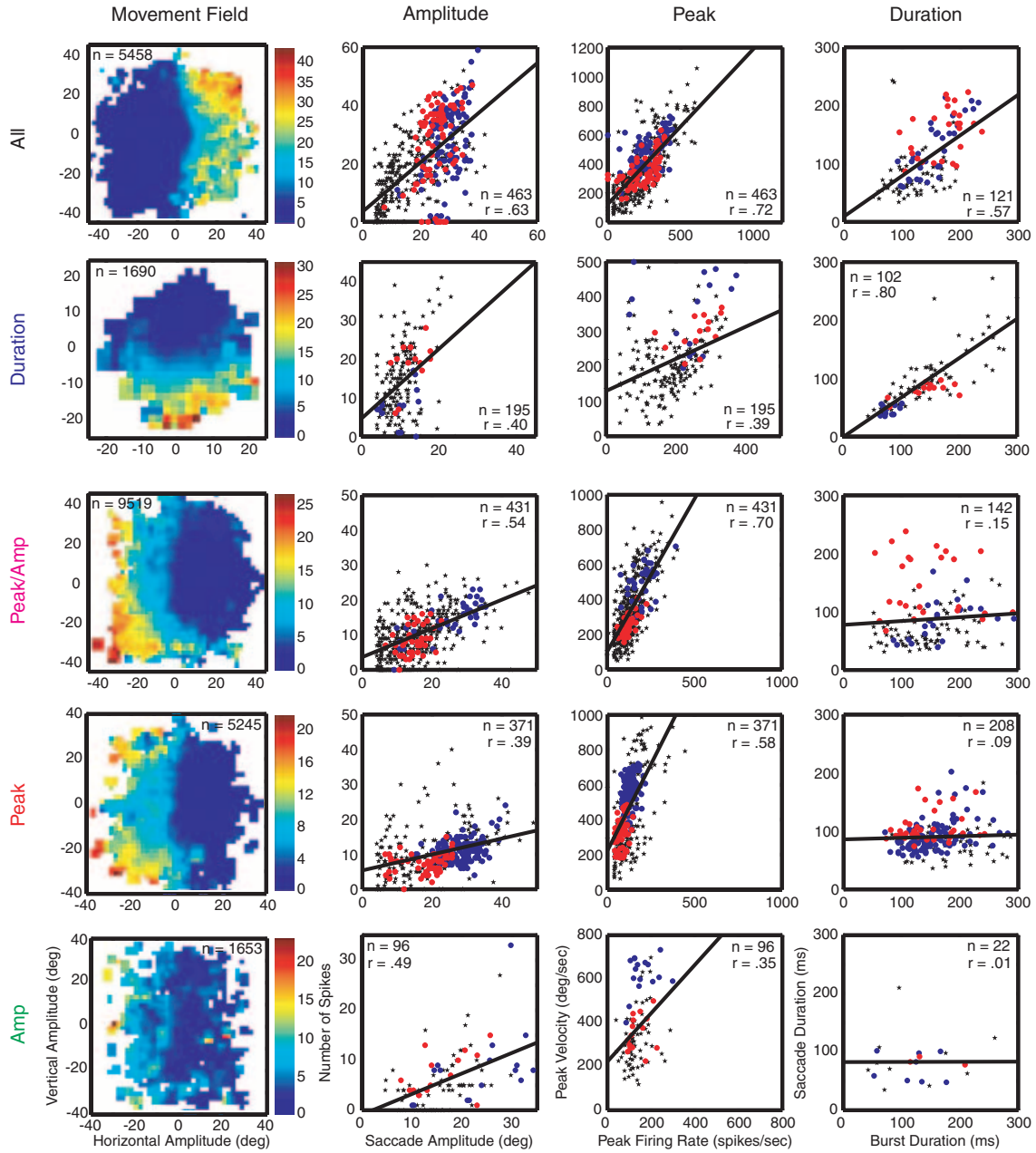

Figure 2. Representative movement fields & metrical relationships
The movement fields and corresponding analysis of the three tested metrical relationships (amplitude, peak and duration) plotted for five representative cMRF neurones. Column 1: movement fields display spike number as a function of saccade direction and amplitude as if the eyes had started at primary position (i.e. in retinotopic coordinates) with warm colours (orange, red) indicating a higher average number of spikes than cool colours (blue, green). Areas in white were unsampled. Column 2: iso-direction plots along the optimal direction of each cell showing the 'Amplitude' relationship (number of spikes *versus* saccade amplitude) for VG (blue dots), MG (red dots), and all other saccades (black stars, including spontaneous saccades and saccades to the fixation light). Column 3: the 'Peak' relationship (peak velocity *versus* peak firing rate) and Column 4: 'Duration' relationship (saccade duration *versus* burst duration) for saccades along the optimal direction. Each example neurone appears to be better related to one or more saccade metrics (row label). Axis labels in the bottom row apply to the columns above.

in Fig. 3. Notice that the correlations for an individual saccade metric (i.e. amplitude, peak or duration) across the entire sample of neurones were widely distributed and did not suggest an obvious grouping of neurones. However, when examining neurones independently, it appeared that individual cells were well correlated to one or more different metrics (Fig. 2, rows). This approach suggested that an analysis across the three relationships might uncover logical groupings of neurones based on their correlations to all of these metrics.

We defined *a priori* eight categories based on the three metrics into which each neurone could be placed. An individual neurone could be related to any single metric ('Amplitude', 'Peak', 'Duration'), any two metrics ('Peak/Amp', 'Peak/Duration', 'Duration/Amp'), all three metrics ('All'), or no metrics ('None'). These eight possibilities are represented on the Venn diagram in Fig. 4*A*. To identify whether the neurones actually fell into any separate grouping based on their metrical correlations, we employed two methods of cluster analysis. The primary motivation for using cluster analysis was the ability to identify possible groupings of cells in an objective way. As a result, inclusion into a specific group was independent of level of correlation and did not force cells into the predefined groups. Another advantage of cluster analysis was its insensitivity to the variability in the data used to establish the correlation coefficients (i.e. measurements of different saccade metrics could contain different levels of noise).

A hierarchical algorithm using Euclidean distances and Ward's method of amalgamation produced eight clusters (Fig. 4*B*). These eight categories were similar, but not identical to those we defined *a priori*. For example, hierarchical clustering identified no cells that fell into the 'Peak/Duration' or 'Duration/Amp' categories, but identified two groups of cells related to 'All' metrics (a very highly correlated group and a well correlated group). To explore whether a different number of clusters might better represent the data, we tested other distance and amalgamation methods and assessed how well they fitted the dataset by comparing their cophenetic correlation coefficients (see Methods). The hierarchical clustering with the optimal fit (i.e. highest cophenetic correlation coefficient, $c = 0.89$) suggested that a grouping into seven sets was optimal. The reduction in cluster number was the result of a combination of the two groups that each had high correlation coefficients to all three metrics (i.e. with seven clusters there was only one 'All' group instead of two). Likewise, clustering using a k-means algorithm (a non-hierarchical method) produced the smallest number ($n = 0$) of mis-clustered cells (silhouette value < 0) and largest mean silhouette value (0.51) with seven clusters (Fig. 4*C*). Therefore, we grouped the cells based on these seven k-means clusters.

Recall that inclusion into each of the groups defined by this method is not based on an arbitrary level of correlation coefficient (e.g. $r > 0.5$). Therefore, it was interesting that when the average correlation for each of the three metrics was plotted for each of the seven groups (Fig. 4*D*), the groups corresponded closely with those we defined *a priori* (Fig. 4*A*). Using the cluster groups in conjunction with the average correlation coefficients we identified the following categories. Just under one-fifth of the cells (cluster 1) were well correlated to all three metrics ('All', 18%, $n = 11$). One third ($n = 19$) of cMRF neurones had a burst duration that was correlated to saccade duration, including a group of neurones whose discharge was better correlated to duration than saccade peak velocity or amplitude (cluster 2, 'Duration', 13%, $n = 8$). Many neurones also exhibited a relationship to peak velocity, either in combination with a high correlation to amplitude (cluster 3, 'Peak/Amp', 20%, $n = 12$) or with only a weak amplitude relationship (cluster 4, 'Peak', 20%, $n = 12$). In yet another group, cells had a preferential correlation to

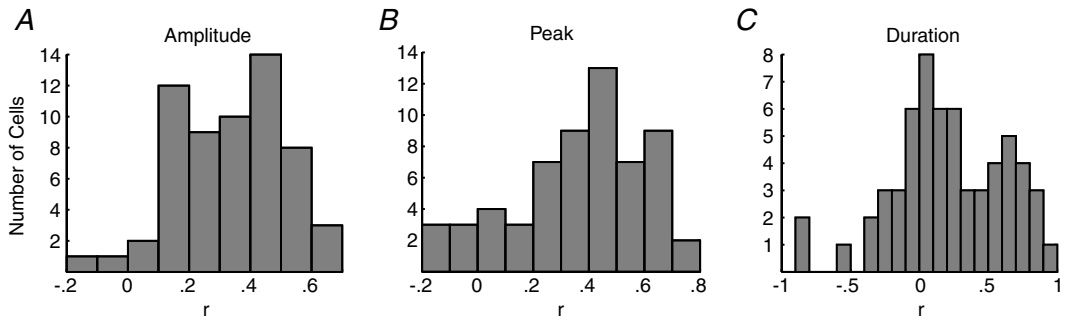

Figure 3. Metrical relationships for the population
Histograms of the population of correlation coefficients for each metrical relationship examined (*A*, Amplitude; *B*, Peak; *C*, Duration). All bins are 0.1 wide. No grouping of the cells was apparent for any of the individual relationships. In other words, there appeared to be a continuum from very weak correlations to strong positive correlations for each of the metrics. Three cells had strongly negative correlations to duration, but none of these correlations was significant ($P > 0.05$).

amplitude with only a weak relationship to peak velocity (cluster 5, 'Amp', 10%, $n = 6$). Finally, 18% ($n = 11$) of cells displayed no relationship to saccade metrics (clusters 6 and 7, 'None'). These cells were predominantly those that had less robust activity around the time of the saccade and no clear movement field. Note that both clustering algorithms identified one group of three cells that had highly negative correlations to duration (cluster 7, 'None (− Dur)'. Upon further examination, we found that none of the correlations in cluster 7 were significant ($P < 0.05$) and the cells did not display any characteristics inversely related to duration (such as pausing during saccades). Therefore, these cells were not considered for additional metrical analysis.

To confirm that the cluster analysis had identified recognizable groups of neurones, we examined the clusters in three dimensional space, where a clear relationship of individual cells to the various metrics became apparent (Fig. 5 shows three 2-D plots). For example, when the correlations to saccade amplitude and peak velocity were

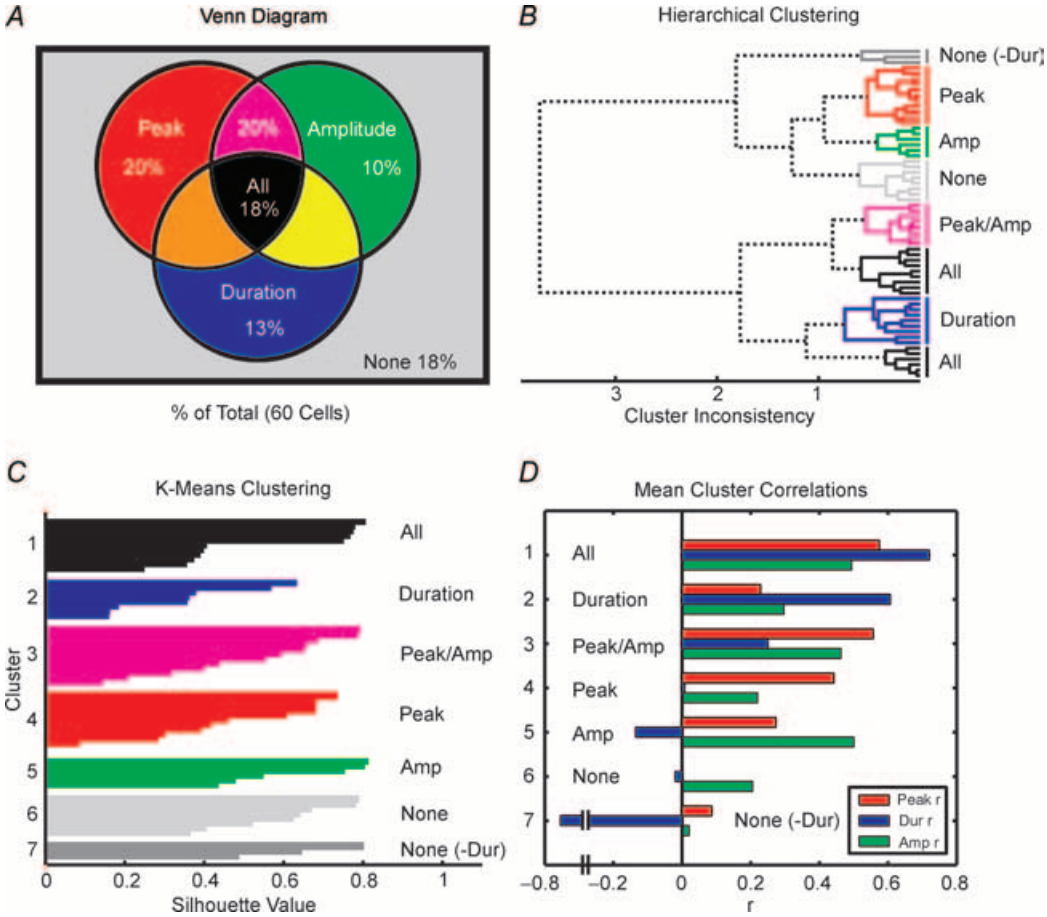

Figure 4. Categorization of cMRF neurones based on metrical relationships
Each cMRF neurone was tested for three metrical relationships: (1) number of spikes *versus* saccade amplitude (Amplitude); (2) peak saccade velocity *versus* peak firing rate (Peak); and (3) saccade duration *versus* burst duration (Duration). *A*, the Venn diagram displays the eight possible categories defined *a priori* ('Amplitude', 'Peak', 'Duration', 'Peak/Amp', 'Peak/Duration', 'Duration/Amp', 'All', 'None') that could contain neurones based on the combination of relationships to the three metrics (each circle represents a relationship to one metric). Neurones that had strong correlations to more than one metric fall within multiple circles, with those matching all three in the centre of the diagram. Those neurones lacking a correlation to any of the metrics would fall outside the circles. Actual per cent of cells from the total sample (60 neurones) falling into the categories were defined by cluster analysis. *B*, dendrogram of hierarchical clustering based on Euclidean distances and Ward's method of amalgamation separates the neurones into eight groups. These groups are similar, but not identical, to those defined *a priori* in *A*. *C*, k-means clustering on the optimal number of clusters (seven) returned similar results, except there was only one 'All' group. Silhouette values indicate the strength of fit for each data point into its defined cluster, 1 being the most distinct fit, values < 0 being an inappropriate clustering. *D*, mean correlations of the three metrics in the groups defined by the k-means analysis produced categories similar to those predicted *a priori*. Note that no cluster represented cells with a combination of 'Peak/Duration' or 'Duration/Amp' relationships. Instead, cells with these properties always had strong correlations to all three metrics and folded into the 'All' group.

considered together (Fig. 5*C*), cells with a high correlation to both parameters were evident (squares and upward triangles). However, when the duration relationship was also considered (Fig. 5*A* or *B*), it was obvious that some of these cells also had a strong duration relationship (squares – the 'All' group) while the others did not (upward triangles – the 'Peak/Amp' group). Thus, the cluster analysis demonstrates that only when the static measures of the relationships of neuronal discharge to amplitude, duration and peak velocity were considered *together* was the type of information carried by each cell understood.

Relationship to instantaneous eye velocity

We predicted that cMRF cells whose discharge was well correlated to saccade peak velocity and duration using static measures would display evidence of a relation to instantaneous saccade velocity. This idea was qualitatively demonstrated by a neurone whose discharge was closely associated with all three saccade metrics (Fig. 6). The movement field (Fig. 6*A*) shows that this cell fired before all contralateral (leftward) movements. We selected eight leftward saccades of increasing amplitude across this movement field (Fig. 6*B*). Saccade velocity, the spike density function, and unit activity for each of these movements were further expanded in Fig. 6*C*. Note that for each of the eight saccades, including the two saccades with a prolonged deceleration (the 27 and 30 deg saccades), the spike density and saccade velocity waveforms are nearly identical over time. This suggested that neurones of this type had an underlying relationship to instantaneous eye velocity.

If this were indeed the case, then the firing rate of these neurones should change dynamically in relation to changes in saccade velocity. However, during saccades of a single behaviour (e.g. visually guided saccades, Fig. 7), amplitude and peak velocity co-vary in a stereotyped 'main sequence' (Fuchs, 1967),

$$\text{peak velocity} = a * (1 - e^{-\text{amp}/b})$$

where a represents the asymptotic (maximum) peak velocity and b is a constant. Hence, saccades of a single behaviour usually show little variance in velocity profile for a given amplitude (e.g. see Fig. 1*A*, 2nd row, Velocity). Thus, we incorporated the memory guided saccade (MG) protocol into a monkey's behaviour repertoire to expand the range of eye velocities and durations generated for saccades of particular amplitude (Fig. 7) and assessed the results using a dynamic analysis.

Dynamic analysis

To quantify the relationship between instantaneous eye velocity and cell discharge in the group of neurones with a metrical relationship, we utilized a dynamic analysis method previously described (Cullen *et al.* 1996). If the discharge of cMRF neurones was most closely tied to some aspect of eye velocity (instantaneous, peak, duration, etc.), we should be able to predict the firing rate of a neurone during VG saccades based on a model developed from the observed firing rate during the MG saccades and vice versa. A sample comparison of individual traces of VG and MG saccades with matching amplitude and

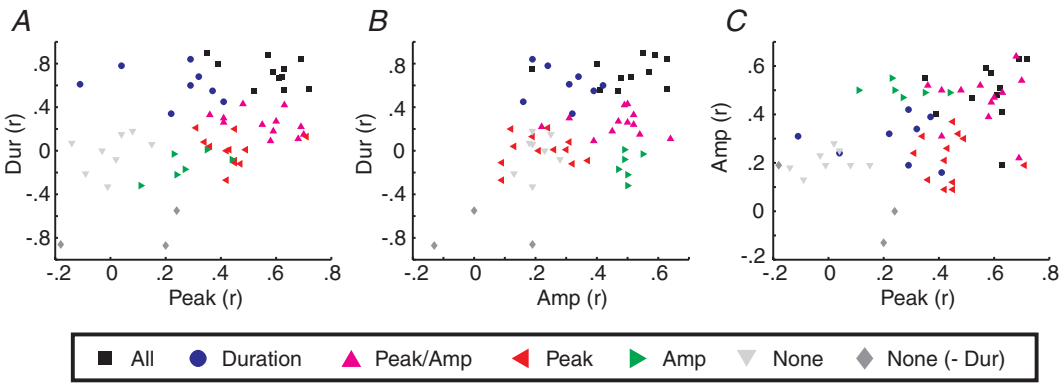

Figure 5. Visualization of neuronal clusters
A–C, scatter plots of the correlation coefficients for two of the three tested relationships. Cells were grouped (coloured symbols) based on k-means clustering across all three metrical relationships. Obvious clusters occurring in three dimensions can be viewed here in two dimensions by following each group across the three plots. For example, red left facing triangles (centre of *B*) represent a cluster of cells related to peak saccade velocity but lacking strong correlation to saccade duration or amplitude. In *B* when peak velocity is not considered, these cells cluster with 'None' cells (grey downward triangles) that are not related to any metric. However, in *A* or *C* when the peak relationship is considered, these cells are clearly distinct from the 'None' cells and may cluster with other cell groups depending on the metrical correlations being displayed.

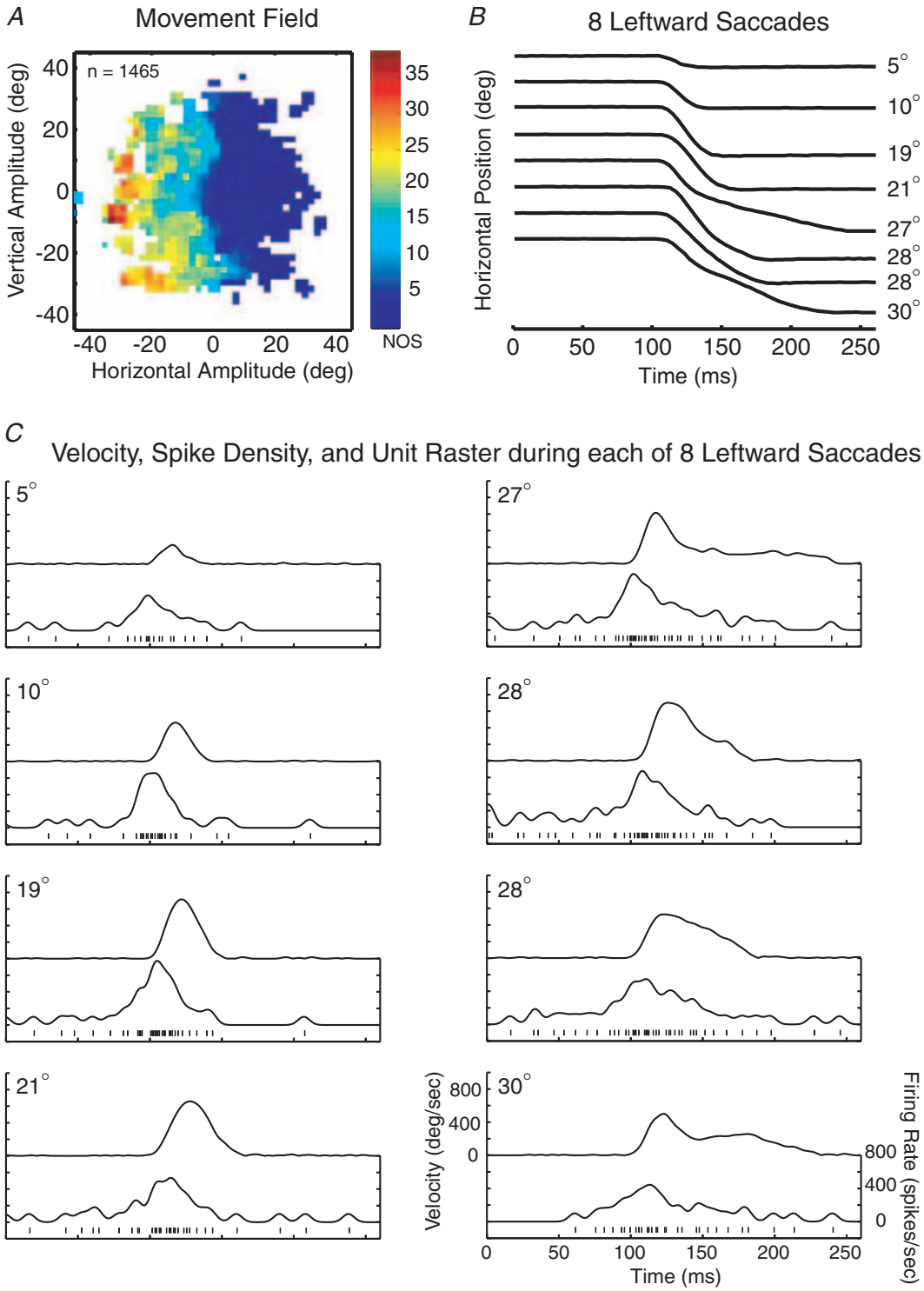

Figure 6. Instantaneous eye velocity-related cell
A, the movement field of a cMRF neurone that was active for all leftward movements. This cell had strong relationships to all three saccade metrics. *B*, eight purely leftward saccades of increasing amplitude recorded while holding the neurone. *C*, the velocity, spike density function and unit activity corresponding to each of the eight leftward saccades. Note that cell activity closely corresponds to saccade velocity for the duration of the saccades on an individual trial basis. Labels in *C* refer to the amplitudes in *B*.

direction is shown in Fig. 8*A*. Note the lower peak velocity and longer duration of the MG saccade (Fig. 8*B*, light grey trace) as compared with the VG saccade velocity (Fig. 8*B*, dark grey trace). This difference in saccade velocity was closely mirrored by the firing rate of the neurone during the two behaviours (Fig. 8*C*). To assess if the cMRF neuronal discharge changed with saccade dynamics across a population of saccades, we computed the optimal dynamic model for the population of VG and MG saccades, respectively (see Methods). These optimal models (continuous black lines) were compared with the actual firing rates in Fig. 8*D* (VG) and Fig. 8*E* (MG).

Next, we tested our ability to predict the firing rate in one behaviour using the model developed from saccades made with the alternative behaviour (dashed black lines). For example, a predicted model of the firing rate during VG saccades was created using the instantaneous eye velocity observed during the VG saccades with model terms optimized during MG saccades. For this cell, the VAF was the *same* regardless of whether the predicted or optimal model was fitted to the data. The similar scaling of the optimal and predicted models means that the b parameters, which adjust the gain of the velocity, were virtually identical between the behaviours ($b_{VG} = 0.50$, $b_{MG} = 0.48$). The offset observed between the optimal and predicted firing rate models (note that the offset along the ordinate does not influence the VAF) was due to the change in the bias parameter during the VG and MG saccades ($a_{VG} = 142$, $a_{MG} = 48$). This offset indicates that while the cells may encode saccade metrics in their burst, other factors may influence the underlying background activity of these cells. This is not surprising since the background rate of cMRF neurones has been previously shown to be influenced by attention, fixation and vision (Waitzman *et al.* 1996).

We carried out this comparison of VG and MG saccades in the subset of neurones with a metrical relationship that had sufficient VG/MG data (27 of 49 cells). Regardless of background activity, models of predicted firing rate using one behaviour (MG) were very close to the optimal VAF established using the other behaviour (VG) in those cases where velocity models had a reasonable fit to the data (VAF > 0.2) (Fig. 8*F*, all symbols). The fact that the dynamic models could be used interchangeably indicates that the changes in the temporal firing pattern of these cMRF neurones were the result of the difference in saccade dynamics induced by each of the behaviours. Moreover, this result supports the idea that the metrical relationship found in one behaviour was conserved in the alternative behaviour. This is why the predicted and optimal VAFs fall along the line of unity. This was also seen in Fig. 2 where VG and MG saccades fell along the same line of correlation (compare blue *versus* red dots). Had predicted models not matched closely with the optimal models, it would have suggested that cMRF neurones were influenced by other aspects of the behaviours rather than changes in saccade dynamics (e.g. Stanford & Sparks, 1994).

It is important to note that while the optimal and predicted models were similar, the overall VAF for many of these cells was rather weak. We predicted that dynamic models of eye velocity would account for a large amount of variance of the neuronal discharge for those cells that were related to instantaneous velocity. Vice versa, we predicted that neurones with metrical relationships confined solely to peak velocity or duration would have a poor correlation with instantaneous velocity. Therefore, the dynamic models would account for less variance in the firing rate of these neurones. We tested this prediction by categorizing the VG/MG comparisons based on saccade metrics (Fig. 8*F*, individual symbols). In addition, we performed a dynamic analysis across *all* saccades (including spontaneous saccades) for the iso-direction set of each of the 49 neurones associated with saccade metrics. The results are shown by plotting each cell according to its VAF while retaining its categorization by metric (Fig. 9).

As we suspected, those neurones with the highest VAFs from dynamic models of eye velocity (Figs 8*F* and 9) were well correlated to multiple saccade metrics and were the same neurones whose discharge was more closely associated with instantaneous saccade velocity (e.g. cells of Figs 1 and 6). A cell with either a relationship to saccade peak velocity or duration alone could have a moderate VAF (range of 0.2–0.35), but a combination of metrical relationships was usually required to generate a higher VAF

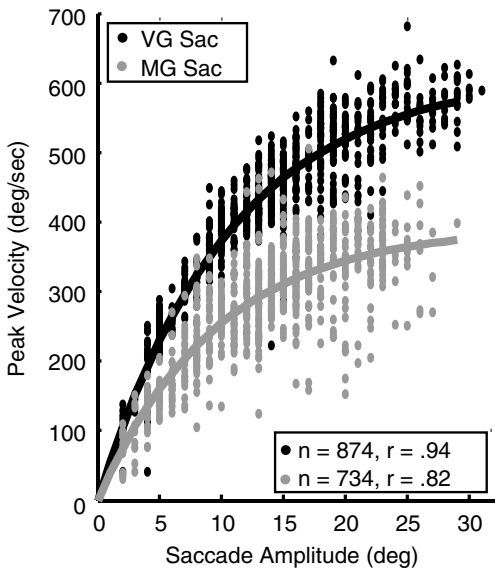

Figure 7. Behavioural protocols alter saccade dynamics
Main sequence plots of VG (black) and MG (grey) movements for one monkey. Plots are fitted with the main sequence equation (see text, $a_{vg} = 614$, $b_{vg} = 11$, $a_{mg} = 393$, $b_{mg} = 10$). Note that for any given amplitude, MG saccades have lower peak velocities than VG saccades. Consequently, the durations of MG saccades are longer than the durations of VG saccades. Thus, use of the MG protocol allowed altered saccade dynamics for saccades of given amplitude.

(0.35 or greater). Note that while some peak (and many peak/amp) cells had strong VAFs, most often these cells were at least weakly correlated to duration. It was possible, however, for a large amount of the variance in the firing rate of cells with an especially strong peak velocity relationship to be accounted for by the velocity models. In general, a high VAF indicated a close relationship to instantaneous velocity while a moderate VAF suggested a relationship to a single eye velocity metric (e.g. peak or duration).

Discussion

This study applied two complementary approaches to analyse a large group of neurones in the cMRF to decide if their properties supported three proposed models of cMRF function in saccadic control. Indeed, the results provide evidence that the discharge of subsets of cMRF neurones: (1) encode instantaneous eye velocity; (2) are related predominantly to saccade duration and not other saccade metrics; and (3) have a spectrum of relationships to saccade dynamics. Therefore, cMRF neurones may subserve the roles hypothesized by these models. In addition, it is clear from this analysis that cMRF neurones display a far greater diversity of neuronal characteristics related to saccades than previously recognized. In the remainder of the discussion, we first address whether grouping cMRF neurones is appropriate. We then expand on the subsets of identified neurones, how these sets correspond to neurones described in previous studies, and how these neurones could participate in saccade control.

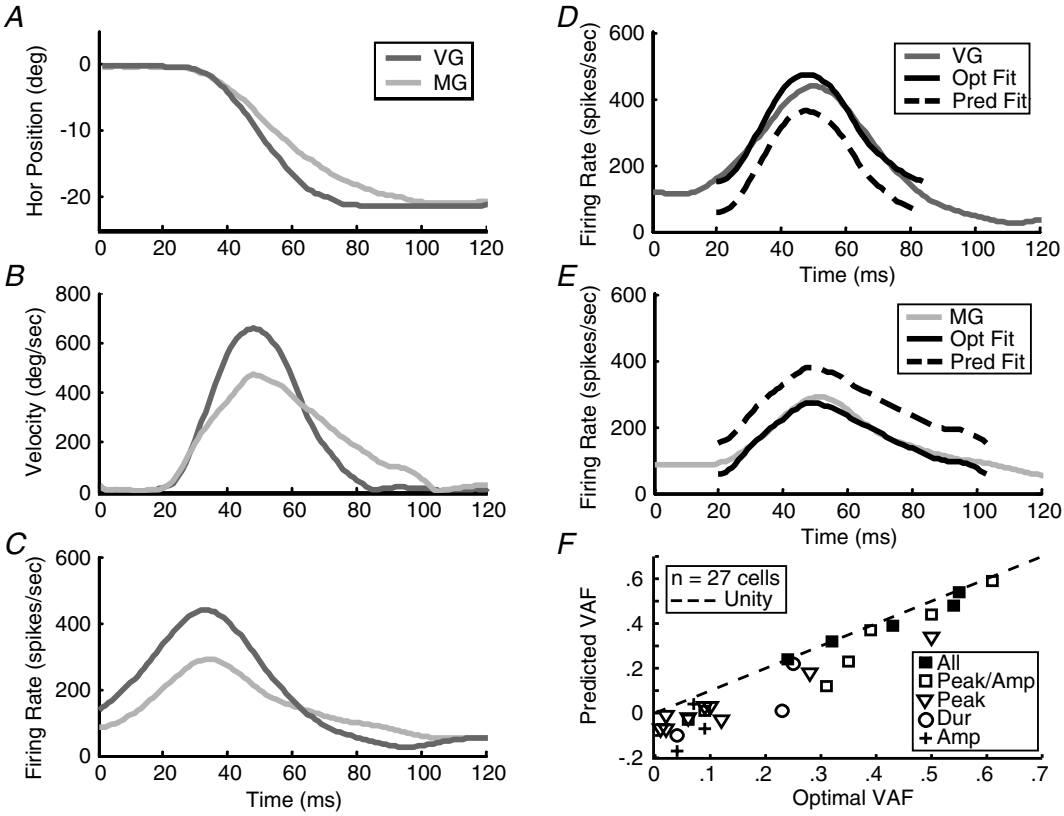

Figure 8. VG/MG comparisons
A, single rightward VG and MG saccades of matching amplitude. *B*, the MG saccade has a lower peak velocity and longer duration than the VG saccade. *C*, the firing rate of the cell changed in conjunction with the instantaneous velocity of the two movements. Note the lower peak firing rate and prolonged discharge of the cell during the MG saccade. *D*, the firing rate during the VG saccade is shifted by the dynamic latency (*td*) of 17 ms and plotted with the mathematically optimal fit for the population of VG saccades (black line) and the predicted firing rate based on VG velocity and the *a*/*b* parameters from the MG model (dashed line). Model *a* parameters are different causing a displacement along the ordinate axis, but *b* parameters and VAF are the same between the optimal and predicted models. *E*, the firing rate of the cell during the MG movement overlaid with optimal and predicted fits. *F*, comparison of the VAFs from the optimal and predicted fits across our VG/MG comparisons population (27 cells). A prediction with a VAF as good as the optimal would fall on the line of unity (dashed line). For cells with reasonably high VAFs (> 0.2), we were able to accurately predict the firing rate during VG saccades based on the models created during MG saccades. This indicates that the difference in firing rate across the behaviours is due to the difference in dynamics between VG and MG saccades. Cells with multiple metrical relationships ('All', 'Peak/Amp') are more likely to be related to instantaneous velocity (fall farther right on the graph).

Selection of cell grouping

An important question related to the analysis we presented is whether the cMRF neurones actually fall into distinct groups. We addressed this question by employing two methods of cluster analysis on the correlation coefficients from the three possible metrical relationships (i.e. amplitude, peak and duration). While cluster analysis provides a more objective method to explore potential groupings amongst data, selecting the number of groups using such methods is not straightforward. The final decision of how many groups to choose is an estimation which can be influenced by the *a priori* bias of the investigator (Everitt, 1993). We attempted to determine the most appropriate number of clusters for the data by comparing either cophenetic correlation coefficients (during hierarchical clustering) or silhouette values (during k-means clustering) (see Methods).

The results of both of these analyses indicated that a grouping of cells into seven clusters was most appropriate (Fig. 4*C*). In retrospect, we noted that these seven clusters matched well with the data we observed (Fig. 2) and the groupings we identified *a priori* (Fig. 4*A*). Furthermore, when we examined the results of clustering, the groups were distinguishable (Fig. 5). While these results provide evidence of distinct relationships amongst different cMRF neurones, we recognize that cells may not rigidly fall into isolated groups. For example, almost all cells that were related to one of the metrical properties had a least a weak relationship to the other metrics (Figs 4*D* and 5). Furthermore, while k-means clustering produced very high silhouette values within the seven clusters (most clusters approach 0.8), a number of the group members had lower silhouettes (< 0.4) indicating possible overlap between the groups.

Another important result of the cluster analysis was that no groups were identified that fell into the *a priori* predicted categories with 'Peak/Duration' or 'Duration/Amp' relationships. Instead, clustering suggested that cells with these relationship combinations were better associated with the 'All' group. This is intuitive, since it is hard to imagine a cell having both a peak and duration relationship, but also lacking a relationship to saccade amplitude. However, such a distinction would have been missed if cluster analysis was not employed. We suggest that the classification we provide is a reasonable grouping that highlights potential differences in the encoding of cMRF neurones and lays a framework for exploring potential channels of information flow in saccadic control. However, future work may be able to refine this categorization.

Movement fields

In a recent study in non-human primates free to move their heads, Pathmanathan *et al.* (2005*b*) classified cMRF neurones into three groups of movement fields: (1) monotonically open, (2) non-monotonically open, and (3) closed, and estimated that approximately one third of sampled neurones fell into each category. In the current analysis, we found the majority of our sampled neurones fitted the pattern of the monotonically open cells. However, the discharge of many of the previously identified non-monotonically open or closed neurones did not begin to decline until the monkey had made gaze saccades of amplitudes greater than 35 deg. Therefore, it is possible that neurones in our study that appear to be monotonically open within our ± 35 deg range of recording would have been classified as non-monotonically open or closed had we recorded gaze shifts of larger amplitude. This is supported by the fact that most prior cMRF studies, none of which included gaze shifts of large amplitude, also report a majority of neurones whose properties were consistent with monotonically open movement field cells (Moschovakis *et al.* 1988*b*; Handel & Glimcher, 1997).

One of the more surprising findings of the current study was the evidence that many of the monotonically open movement field cells did not have a *highly* correlated NOS/amplitude relationship. Instead, these neurones were preferentially related to velocity or duration (Fig. 2). Thus, the definition of open movement field cells must be expanded to encompass not only cells with monotonically increasing spike number with saccade amplitude but other cells with relationships to saccade velocity and duration. For example, cells with a relationship to peak eye velocity could have a monotonic increase in discharge up to specific saccade amplitude, after which their discharge would plateau (i.e. velocity main sequence). Therefore

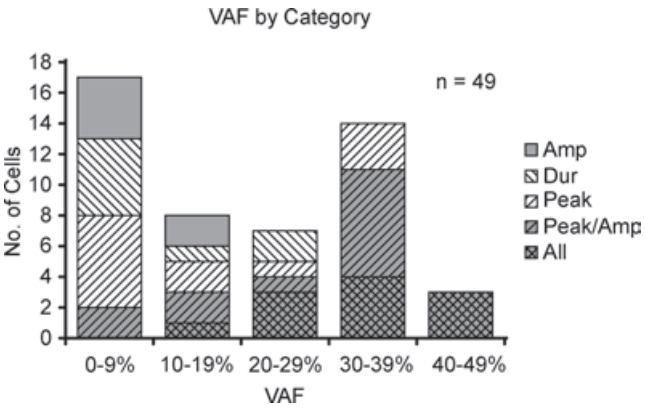

Figure 9. VAF by metrical category
The VAF for dynamic models of eye velocity fitted to the firing rate for *all* saccades along the optimal direction is plotted for each of the 49 cells with a metrical relationship. The plots preserve the metrical category to which each cell belonged (from k-means clustering). The categories are plotted such that the combination of the background fill pattern for the individual metric relationships (i.e. amplitude, duration and peak) is used to create the fill for those categories with more than one metric. Those cells with the highest VAF have a relationship to multiple saccade metrics and are the same cells that were related to instantaneous eye velocity.

future studies will have to sub-classify open movement field neurones with respect to a particular metric. This realization has implications for neuronal mechanisms of saccade control.

Saccadic control channels

A primary function of the saccadic system is to accurately reposition the eyes onto targets of interest (Zee *et al.* 1976). Thus, even when saccade velocity is severely reduced, either by lesions (e.g. Schiller *et al.* 1980; Lee *et al.* 1988) or by drugs (e.g. Jürgens *et al.* 1981), the resulting slow saccades remain accurate. This has suggested that amplitude is one of the fundamentally controlled variables within the oculomotor system. Indeed, the NOS/amplitude relationship is usually the strongest reported metrical relationship for the EBNs (Moschovakis *et al.* 1996). However, there is evidence that the NOS emitted by an EBN is indirectly controlled via independent mechanisms regulating saccade duration and velocity (Moschovakis *et al.* 1996). Our results suggest that independent pathways related to different aspects of saccade metrics and dynamics may be crucial for saccade control. At least three of these channels (amplitude, velocity and duration) are evident in our data.

Amplitude cells

Two groups of cMRF neurones identified by metrical analysis had a relationship to saccade amplitude but not duration ('Amp' and 'Peak/Amp' groups). This finding is not surprising, since a group of reticulo-tectal neurones in the cMRF that had a strong relationship to saccade amplitude but lacked a duration relationship has been previously described (Moschovakis *et al.* 1988*b*). Thus, by virtue of projections to the SC, such cMRF neurones could provide a feedback signal of amplitude. Feedback of the current change in eye position has been proposed as one method for maintaining saccade accuracy (Jürgens *et al.* 1981) and loss of this signal could explain the hypermetric saccades observed following inactivation of the cMRF (Waitzman *et al.* 2000). A separate set of amplitude-related cells have also been previously identified in the cMRF (Scudder *et al.* 1996), which project downwards to the OPNs, IBNs and other pontine and medullary oculomotor control areas. Thus, amplitude-related cells could participate in either feedback or feed-forward saccade control.

Velocity cells

A majority of cMRF neurones had a relationship between peak firing rate and peak saccade velocity (68%). This confirmed previous evidence of a velocity relationship in a subset of cMRF neurones (Waitzman *et al.* 1996). However, the current study provides further insight into the specific coding properties of these cells. In particular, some cMRF neurones were correlated only to peak saccade velocity while others were related to instantaneous eye velocity.

Under normal conditions, saccade-related burst neurones in the SC lack a relationship to saccade velocity (Wurtz & Goldberg, 1972; Sparks, 1975). Since the cMRF receives a significant afferent input from the SC, it is unclear how such a velocity relationship could arise within the context of synapses coming from the activated portion of the tectum. A feed-forward anatomical mechanism has been postulated to accomplish a similar conversion via the connections from the SC to the EBNs (Grantyn *et al.* 2002, 2004). Thus, one possibility is that the pattern, weighting and density of projections from the SC to the cMRF cause the cMRF neurones to develop temporal characteristics (see spatial to temporal transform below). Another source of the velocity signal in cMRF neurones could be from portions of the PPRF. For example, feedback from EBNs and IBNs to the SC and higher oculomotor structures could be mediated via the cMRF (Waitzman *et al.* 1996). This idea is supported by reticulo-reticular connections from the pons to the cMRF (Graybiel, 1977; Büttner-Ennever, 1988). Velocity feedback through the cMRF could also explain the evidence of a saccade velocity relationship observed in some SC neurones following inactivation of the OPNs (Soetedjo *et al.* 2002).

In a feed-forward role, cMRF neurones with a relationship to either peak or instantaneous eye velocity could provide an additional channel of velocity control to the EBNs or IBNs that parallels the direct tecto-pontine pathway. Alternatively cMRF neurones carrying an instantaneous eye velocity signal could target the OPNs in the pons (Büttner-Ennever, 1988; Langer & Kaneko, 1990; Scudder *et al.* 1996). There is recent evidence that OPN discharge is eye velocity dependent (Yoshida *et al.* 1999) and that the inhibition of the OPNs due to SC activation is relayed via an intermediate group of neurones (Yoshida *et al.* 2001). Thus, those cMRF neurones related to instantaneous eye velocity could serve to latch the OPNs off during saccades.

Duration cells

The analysis of saccade metrics also identified one set of cMRF neurones whose discharge was preferentially associated with saccade duration (13%). This previously unrecognized group of neurones fitted the profile of those proposed by Soetedjo *et al.* (2002). We hypothesize that connections between the SC, cMRF and OPNs comprise a duration channel. For example, to initiate a saccade, target selection information excites closed movement field cells in the SC motor layer specifying the desired gaze displacement. These SC neurones in turn could excite duration cells in the cMRF. As suggested by Soetedjo *et al.* (2002), positive, recurrent feedback from the cMRF

maintains excitation in the SC until it is shut down by inhibition arising from the OPNs. This circuitry would maintain the SC target selection signal for the duration of the saccade.

Unlike the schema suggested by Soetedjo *et al.* (2002), we propose that duration cells in the cMRF need not exactly reflect the movement field properties of the SC (i.e. spatially coded, closed movement field cells) to provide duration feedback. Instead, this feedback could be provided by open movement field, duration-related cMRF neurones. Therefore, it is not necessary for the cMRF duration cells to undergo an explicit 'reverse' transformation from temporal to spatial encoding. These cells could receive input from multiple areas of the SC map and in turn send recurrent collaterals back to multiple SC cells. Local inhibition within the burst layer of the SC or internal cellular properties could prevent activation of non-selected SC neurones through recurrent feedback. In this way, a single group of open movement field, duration only cMRF neurones could provide duration feedback to the entire SC. In summary, the input from the cMRF duration cells would be capable of sustaining the firing of the selected group of SC neurones, but would be insufficient alone to drive unselected SC cells (i.e. the drive signal from other regions of the cerebral cortex must be present to initiate a response of the SC cells).

One problem with a scheme in which the cMRF neurones participate in a feedback loop controlled exclusively by the OPNs is that inactivation of the OPNs does not affect saccade accuracy and the duration signal persists in the SC (Soetedjo *et al.* 2002). Therefore, neurones in the cMRF must receive other inhibitory inputs that signal saccade offset (e.g. motor error). This inhibition would be capable of shutting down the SC-cMRF reverberant circuit when the saccade is on target. One possibility is that feedback in the amplitude channel becomes the predominant control loop when OPNs are inactivated.

Cells potentially involved in the spatial to temporal transform

Pathmanathan *et al.* (2005*a*) postulated that cMRF neurones could participate in the development of the temporally coded excitatory burst neurone signal from the spatially coded SC target selection signal. A strict interpretation of the 'spatial to temporal transformation' would state that any neurone with an open movement field and any metrical relationship (i.e. amplitude, velocity or duration) is already temporally encoded and thus cannot play a role in the transformation. However, neurones with a correlation of 0.5 between spike number and saccade amplitude cannot be directly responsible for driving the extra-ocular muscles (Hepp & Henn, 1983). Rather, the brainstem must develop a much more highly correlated 'motor-neurone driving signal' whose temporal characteristics more closely mimic the *dynamics* of the motoneurone (Sylvestre & Cullen, 1999).

How does the brainstem arrive at such stereotypic signals? Hepp & Henn (1983) postulated that the spatial to temporal transformation could occur as a step-wise process. Building on this idea, Pathmanathan *et al.* (2005*a*) suggested that a recursive/hierarchical algorithm was used to increase the temporal correlation of burst neurones. In this scheme, weakly correlated neurones (closed, non-monotonic, or monotonic open movement fields) would project to more strongly correlated neurones with recurrent collaterals participating in the development of finely tuned temporal signals downstream (EBNs) that could drive the eye muscles. Thus, we argue that cells with weak 'temporal' characteristics (i.e. weak correlation coefficients or low VAFs) could play an integral part of the spatial to temporal transform. A similar schema has been previously proposed showing that an intermediate cell layer could facilitate sensorimotor transformations such as the transition from eye centred to head centred coordinates (Pouget *et al.* 2002).

We utilized two approaches in the analysis of cMRF neurones to fully characterize each neurone's relationship to saccades. We found that the varied metrical relationships of cMRF neurones ranging from weakly to strongly correlated to individual saccade metrics had similar firing characteristics to those cells in the middle layer of a three layer model generating temporal characteristics from a purely spatial signal (Pathmanathan & Waitzman, 2003). More importantly, we found that neurones that had multiple metrical relationships (e.g. the 'All' group) had higher VAFs using velocity models. In other words, the cMRF could participate in generating the excitatory drive for the EBNs in a stepwise manner with cells further along the hierarchy more closely replicating saccade dynamics.

The weighting and patterns of connections between the SC and EBNs have already been hypothesized as an important component in the generation of temporal signals (Grantyn *et al.* 2004). A similar mechanism may develop temporal signals in the cMRF. We believe that the spatial-to-temporal transformation is probably a process completed through multiple pathways and multiple mechanisms (anatomical and physiological). As a result, the loss of a single pathway might slow saccades, rather than eliminate them. This idea is consistent with studies showing that lesions or inactivation of the SC did not abolish saccades (Schiller *et al.* 1980; Albano *et al.* 1982; Aizawa & Wurtz, 1998).

Conclusions

We have utilized a number of methods to distinguish and refine the physiological characteristics of different sub-classes of cMRF neurones. These sub-classes of neurones support recently proposed models of cMRF

function. Some of these classes fitted with previously described data while others (e.g. duration cells) represent previously unrecognized neurones. Most likely, neurones in different groups have different roles in saccade control. We suggest that cMRF neurones with metrical relationships to saccade amplitude and velocity subserve dual functions providing both descending amplitude and velocity information to EBNs in the PPRF as well as feeding this information back to the superior colliculus. cMRF neurones carrying instantaneous velocity or duration information may impinge upon the OPNs and subserve a latching function holding them off for the duration of the saccade. At the same time, cMRF neurones whose discharge is solely associated with saccade duration could mediate feedback from the OPNs to the intermediate and deep layers of the SC. Finally, cMRF neurones with amplitude information could provide feedback to the SC about the current change in eye position. It is clear that based on existing data alone, we cannot decide between feedback or feed-forward roles for most individual classes of neurones. If the cMRF is involved in different control streams, identifying the anatomical targets of individual cMRF neurones displaying different physiological properties is critical in defining the role of the cMRF in saccadic control.

References

Aizawa H & Wurtz RH (1998). Reversible inactivation of monkey superior colliculus. I. Curvature of saccadic trajectory. *J Neurophysiol* **79**, 2082–2096.

Albano JE, Mishkin M, Westbrook LE & Wurtz RH (1982). Visuomotor deficits following ablation of monkey superior colliculus. *J Neurophysiol* **48**, 338–351.

Büttner-Ennever JA (1988). *Neuroanatomy of the Oculomotor System*. Elsevier New York, New York.

Chen B & May PJ (2000). The feedback circuit connecting the superior colliculus and central mesencephalic reticular formation: a direct morphological demonstration. *Exp Brain Res* **131**, 10–21.

Cohen B & Büttner-Ennever JA (1984). Projections from the superior colliculus to a region of the central mesencephalic reticular formation (cMRF) associated with horizontal saccadic eye movements. *Exp Brain Res* **57**, 167–176.

Cromer JA, Pathmanathan JS, Dearborn JL & Waitzman DM (2004). The discharge of a subset of mesencephalic reticular formation neurons encodes eye velocity during visually guided and remembered saccades. *Abstr Soc Neurosci* Program No. 880.8.

Cromer JA, Pathmanathan JS & Waitzman DM (2003). Characteristics of central mesencephalic reticular formation (cMRF) neurons during saccades to remembered targets. *Abstr Soc Neurosci* Program No. 79.15.

Cullen KE & Guitton D (1997). Analysis of primate IBN spike trains using system identification techniques. I. Relationship to eye movement dynamics during head-fixed saccades. *J Neurophysiol* **78**, 3259–3282.

Cullen KE, Rey CG, Guitton D & Galiana HL (1996). The use of system identification techniques in the analysis of oculomotor burst neuron spike train dynamics. *J Comput Neurosci* **3**, 347–368.

Everitt B (1993). *Cluster Analysis*. Edward Arnold, London.

Freedman EG & Sparks DL (1997). Activity of cells in the deeper layers of the superior colliculus of the rhesus monkey: evidence for a gaze displacement command. *J Neurophysiol* **78**, 1669–1690.

Fuchs AF (1967). Saccadic and smooth pursuit eye movements in the monkey. *J Physiol* **191**, 609–631.

Grantyn A, Brandi AM, Dubayle D, Graf W, Ugolini G, Hadjidimitrakis K & Moschovakis A (2002). Density gradients of trans-synaptically labeled collicular neurons after injections of rabies virus in the lateral rectus muscle of the rhesus monkey. *J Comp Neurol* **451**, 346–361.

Grantyn A, Moschovakis AK & Kitama T (2004). Control of orienting movements: role of multiple tectal projections to the lower brainstem. *Prog Brain Res* **143**, 423–438.

Graybiel AM (1977). Direct and indirect preoculomotor pathways of the brainstem: an autoradiographic study of the pontine reticular formation in the cat. *J Comp Neurol* **175**, 37–78.

Hallett PE & Lightstone AD (1976). Saccadic eye movements to flashed targets. *Vision Res* **16**, 107–114.

Handel A & Glimcher PW (1997). Response properties of saccade-related burst neurons in the central mesencephalic reticular formation. *J Neurophysiol* **78**, 2164–2175.

Hartigan JA (1975). *Clustering Algorithms*. Wiley, New York.

Hepp K & Henn V (1983). Spatio-temporal recoding of rapid eye movement signals in the monkey paramedian pontine reticular formation (PPRF). *Exp Brain Res* **52**, 105–120.

Judge SJ, Richmond BJ & Chu FC (1980). Implantation of magnetic search coils for measurement of eye position: an improved method. *Vision Res* **20**, 535–538.

Jürgens R, Becker W & Kornhuber HH (1981). Natural and drug-induced variations of velocity and duration of human saccadic eye movements: evidence for a control of the neural pulse generator by local feedback. *Biol Cybern* **39**, 87–96.

Langer TP & Kaneko CR (1983). Efferent projections of the cat oculomotor reticular omnipause neuron region: an autoradiographic study. *J Comp Neurol* **217**, 288–306.

Langer TP & Kaneko CR (1990). Brainstem afferents to the oculomotor omnipause neurons in monkey. *J Comp Neurol* **295**, 413–427.

Lee C, Rohrer WH & Sparks DL (1988). Population coding of saccadic eye movements by neurons in the superior colliculus. *Nature* **332**, 357–360.

Luschei ES & Fuchs AF (1972). Activity of brain stem neurons during eye movements of alert monkeys. *J Neurophysiol* **35**, 445–461.

MacPherson JM & Aldridge JW (1979). A quantitative method of computer analysis of spike train data collected from behaving animals. *Brain Res* **175**, 183–187.

Moschovakis AK, Karabelas AB & Highstein SM (1988*a*). Structure-function relationships in the primate superior colliculus. I. Morphological classification of efferent neurons. *J Neurophysiol* **60**, 232–262.

Moschovakis AK, Karabelas AB & Highstein SM (1988*b*). Structure-function relationships in the primate superior colliculus. II. Morphological identity of presaccadic neurons. *J Neurophysiol* **60**, 263–302.

Moschovakis AK, Scudder CA & Highstein SM (1996). The microscopic anatomy and physiology of the mammalian saccadic system. *Prog Neurobiol* **50**, 133–254.

Munoz DP & Wurtz RH (1995). Saccade-related activity in monkey superior colliculus. I. Characteristics of burst and buildup cells. *J Neurophysiol* **73**, 2313–2333.

Pathmanathan JS, Cromer JA, Cullen KE & Waitzman DM (2005*a*). Temporal characteristics of neurons in the central mesencephalic reticular formation of head unrestrained monkeys. *Exp Brain Res*; DOI: 10.1007/s00221-005-0105-z.

Pathmanathan JS, Presnell R, Cromer JA, Cullen KE & Waitzman DM (2005*b*). Spatial characteristics of neurons in the central mesencephalic reticular formation (cMRF) of head-unrestrained monkeys. *Exp Brain Res*; DOI: 10.1007/s00221-005-0104-0.

Pathmanathan J & Waitzman DM (2003). Functions of the pre-saccadic central mesencephalic reticular formation (cMRF) neurons in spatial to temporal transformation. *Soc for Neuroscience Abstract* **29**, 79.15.

Pouget A, Deneve S & Duhamel JR (2002). A computational perspective on the neural basis of multisensory spatial representations. *Nat Rev Neurosci* **3**, 741–747.

Robinson D (1963). A method of measuring eye movement using a scleral search coil. *IEEE Transactions on Biomedical Electronics*, 137–145.

Rousseeuw PJ (1987). Silhouettes: a graphical aid to the interpretation and validation of cluster analysis. *J Computational Appl Mathematics* **20**, 53–65.

Schiller PH, True SD & Conway JL (1980). Deficits in eye movements following frontal eye-field and superior colliculus ablations. *J Neurophysiol* **44**, 1175–1189.

Scudder CA, Moschovakis AK, Karabelas AB & Highstein SM (1996). Anatomy and physiology of saccadic long-lead burst neurons recorded in the alert squirrel monkey. I. Descending projections from the mesencephalon. *J Neurophysiol* **76**, 332–352.

Silverman BW (1986). *Density Estimation for Statistics and Data Analysis*. Chapman & Hall, London, New York.

Soetedjo R, Kaneko CR & Fuchs AF (2002). Evidence that the superior colliculus participates in the feedback control of saccadic eye movements. *J Neurophysiol* **87**, 679–695.

Sparks DL (1975). Response properties of eye movement-related neurons in the monkey superior colliculus. *Brain Res* **90**, 147–152.

Sparks DL (1999). Conceptual issues related to the role of the superior colliculus in the control of gaze. *Curr Opin Neurobiol* **9**, 698–707.

Sparks DL (2002). The brainstem control of saccadic eye movements. *Nat Rev Neurosci* **3**, 952–964.

Sparks DL & Mays LE (1990). Signal transformations required for the generation of saccadic eye movements. *Annu Rev Neurosci* **13**, 309–336.

Stanford TR & Sparks DL (1994). Systematic errors for saccades to remembered targets: evidence for a dissociation between saccade metrics and activity in the superior colliculus. *Vision Res* **34**, 93–106.

Sylvestre PA & Cullen KE (1999). Quantitative analysis of abducens neuron discharge dynamics during saccadic and slow eye movements. *J Neurophysiol* **82**, 2612–2632.

Waitzman DM, Silakov VL & Cohen B (1996). Central mesencephalic reticular formation (cMRF) neurons discharging before and during eye movements. *J Neurophysiol* **75**, 1546–1572.

Waitzman DM, Silakov VL, DePalma-Bowles S & Ayers AS (2000). Effects of reversible inactivation of the primate mesencephalic reticular formation. I. Hypermetric goal-directed saccades. *J Neurophysiol* **83**, 2260–2284.

Ward RH & Neel JV (1990). Gene frequencies and microdifferentiation among the Makiritare Indians. IV. A comparison of a genetic network with ethnohistory and migration matrices, a new index of genetic isolation. *Am J Hum Genet* **22**, 538–561.

Wurtz RH & Goldberg ME (1972). Activity of superior colliculus in behaving monkey. III. Cells discharging before eye movements. *J Neurophysiol* **35**, 575–586.

Yoshida K, Iwamoto Y, Chimoto S & Shimazu H (1999). Saccade-related inhibitory input to pontine omnipause neurons: an intracellular study in alert cats. *J Neurophysiol* **82**, 1198–1208.

Yoshida K, Iwamoto Y, Chimoto S & Shimazu H (2001). Disynaptic inhibition of omnipause neurons following electrical stimulation of the superior colliculus in alert cats. *J Neurophysiol* **85**, 2639–2642.

Zee DS, Optican LM, Cook JD, Robinson DA & Engel WK (1976). Slow saccades in spinocerebellar degeneration. *Arch Neurol* **33**, 243–251.

Acknowledgements

We would like to thank Dr Jay Pathmanathan for his suggestions, assistance and analysis routines; Dr Paul May for providing expertise in anatomical reconstruction; Drs Kathleen Cullen, Shig Kuwada and Stephen Walsh for their helpful discussion of the data; Dr Douglas Oliver for use of his laboratory facilities and supplies; and Jennifer Dearborn for assisting in experimental recordings and training. Finally, we would like to thank the anonymous reviewers for their insightful commentary and suggestions, which we feel greatly strengthened the final version of this manuscript. This work was supported by NEI grant EY009481, NEI pre-doctoral grant EY015356, and a University of Connecticut Health Center neuroscience training grant NS41224.